doi:10.1038/nature11728

Supplementary Figure S1.

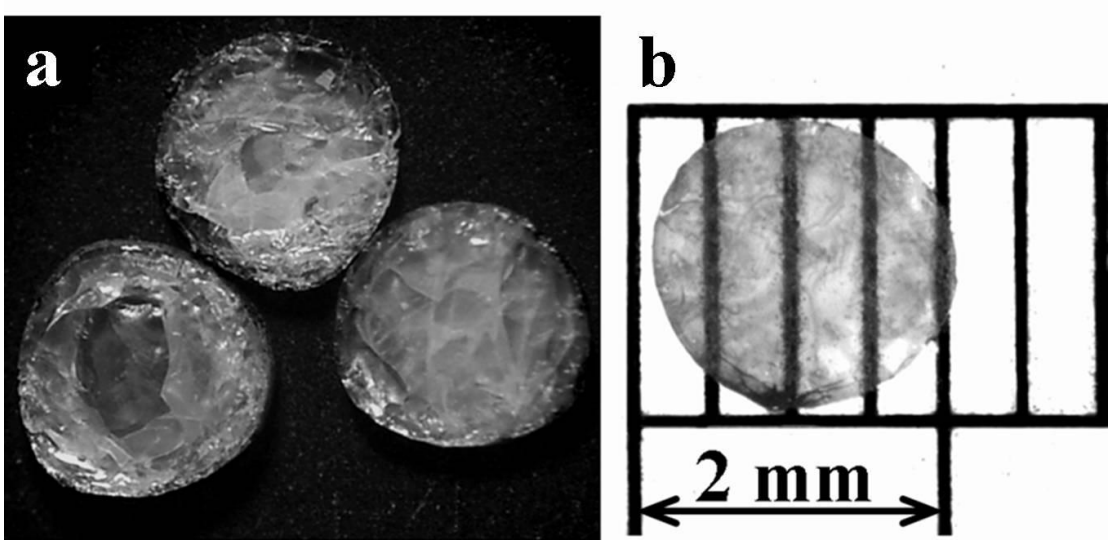

As-synthesized nt-cBN bulk samples with a diameter of ~2 mm. a, Photograph of three as-synthesized nt-cBN samples. **b,** Photograph of an as-synthesized nt-cBN sample over a printed grid, demonstrating its transparency.

Supplementary Figure S2.

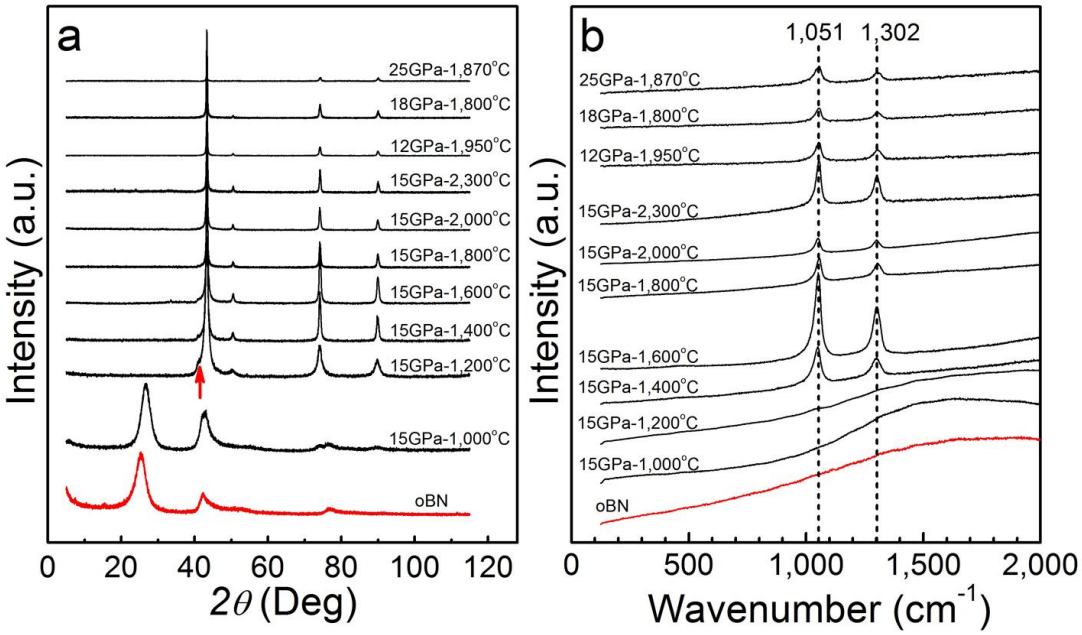

Phase transformations of oBN nanospheres at HPHT. a, XRD patterns after synthesis experiments at various conditions indicated. For starting oBN nanoparticles, the inter-shell spacing calculated from diffraction peak at $2\theta \approx 25°$ is 0.351 nm, larger than the corresponding (002) reflection of hexagonal BN at 0.3328 nm and (003) of rhombohedral BN at 0.334 nm. The sample recovered from 15 GPa and 1,000 °C exhibits an increased intensity for the inter-shell spacing (around 43°), indicating formation of a small amount of cBN. The starting oBN transforms into cBN with a small amount of the wurtzite BN phase (red arrow) between 1,200 and 1,600 °C and then into pure cBN phase above 1,600 °C. **b,** Raman spectra of samples after HPHT synthesis. Above 1,400 °C, two sharp Raman peaks at about 1,051 and 1,302 cm^{-1} are present, which can be assigned to the transverse optical and longitudinal optical phonon modes of pure cBN, respectively.

Supplementary Figure S3.

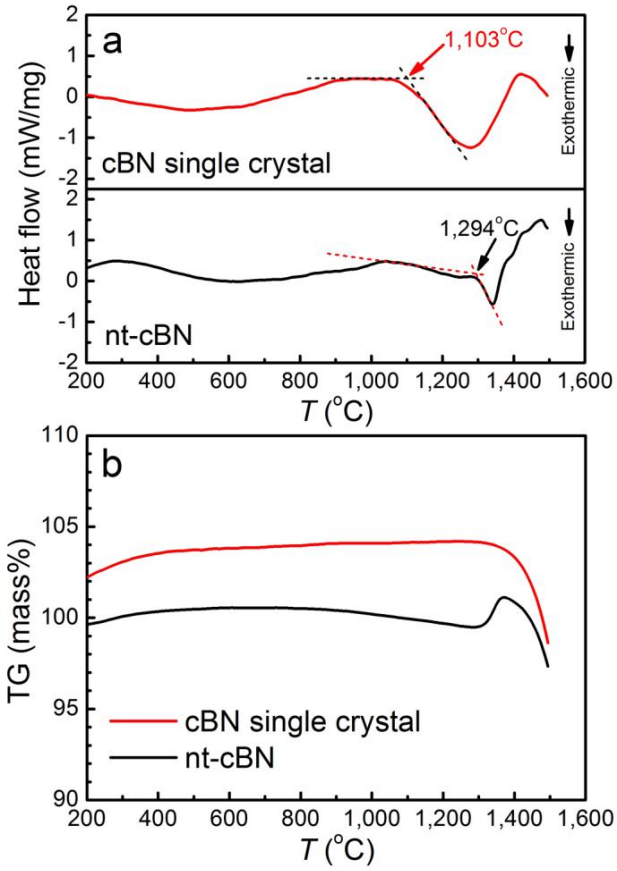

Comparison of oxidation resistance of nt-cBN bulk samples and cBN single-crystal powders in air. a, The onset temperatures of oxidation are determined from the exothermic trough in the heat flow curve measured by DSC. The onset temperature (shown by the change in slope in the heat flow curve) is ~1,103 °C for the cBN single crystals and ~1,294 °C for the nt-cBN bulk. **b,** The corresponding thermogravimetric curves for cBN powders and nt-cBN bulk. Weight gain due to oxidation is greater for cBN powders than for nt-cBN bulk below the onset temperature of oxidation. A weight gain peak, corresponding to the narrow exothermic peak (Fig. S3a), can be seen for nt-cBN bulk, indicating that B_2O_3 (formed during rapid oxidation) is more difficult to evaporate for the bulk due to the reduced ratio of surface to volume.

Supplementary Figure S4.

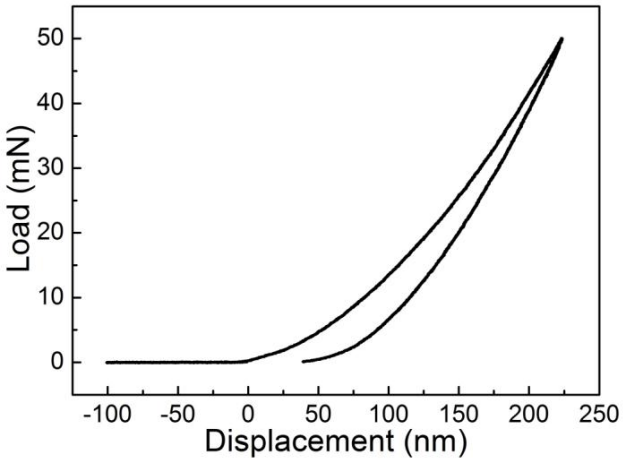

A typical plot of the load-displacement for the nanoindentation measurements of nt-cBN bulk sample. The measured nanohardness H_N and reduced modulus E_r are 97 GPa and 582 GPa, respectively. According to Oliver and Pharr[1], Young's modulus E is determined in nanoindentation measurements by equation $(E_r)^{-1}=(1-\gamma^2)(E)^{-1}+(1-\gamma_i^2)(E_i)^{-1}$, where E and γ are Young's modulus and Poisson's ratio of the sample, while E_i and γ_i are the corresponding parameters for the diamond indenter. In our calculations, E_i=1,141 GPa, γ_i=0.07, and γ=0.121 were used. Thus, the obtained Young's modulus for nt-cBN sample from this curve is 1,164 GPa. From four measurement data listed in Table S1**,** our obtained average value of Young's modulus for nt-cBN is 1,020±213 GPa. The large errors of Young's modulus in our nanoindentation measurements are related mainly to the increased hardness of our sample and the consequently rougher surface finish as shown in the left inset of Fig.3.

Supplementary Table S1.

Samples	H_K±s.d. (n)	H_N±s.d. (n)	E±s.d. (n)
nt-cBN bulk	77.7±3.8 (6)	98.5±11.6 (4)	1,020±213 (4)
cBN crystal, (111) face	44[a]	55[a]	909[a]
ng-cBN bulk (coarse)	40.4[b]	59.7[b]	762[b]
ng-cBN bulk (fine)	49.7[b]	74.9[b]	875[b]
Diamond, (111) face	63[a]	—	1,141[a]
ng-diamond bulk	110-140[c]	62[d]	707[d]

a Experimental data from Ref. 2 and therein.
b Experimental data taking from Ref. 3.
c Experimental data from Ref. 4.
d Experimental data from Ref. 5.

Knoop hardness H_K (GPa), Young's modulus E (GPa), and nanohardness H_N (GPa) of nt-cBN bulk in comparison with cBN and diamond single crystals, as well as ng-diamond and ng-cBN (coarse- and fine-grained) bulks.

References for Supplementary Information

1. Oliver, W. C. & Pharr, G. M. An improved technique for determining hardness and elastic modulus using load and displacement sensing indentation experiments. *J. Mater. Res.* **7**, 1564-1583 (1992).
2. Solozhenko, V. L., Dub, S. N. & Novikov, N. V. Mechanical properties of cubic BC_2N, a new superhard phase. *Diamond Relat. Mater.* **10**, 2228-2231 (2001).
3. Dub, S. N. & Petrusha, I. A. Mechanical properties of polycrystalline cBN obtained from pyrolytic gBN by direct transformation technique. *High Pressure Res.* **26**, 71-77 (2006).
4. Irifune, T., Kurio, A., Sakamoto, S., Inoue, T. & Sumiya, H. Ultrahard polycrystalline diamond from graphite. *Nature* **421**, 599-600 (2003).
5. Couvy, H. *et al*. Nanohardness and Young's modulus of nanopolycrystalline diamond. *Scripta Mater.* **64**, 1019-1022 (2011).